Chapter **II**

ACTIVATED-COMPLEX THEORY: CURRENT STATUS, EXTENSIONS, AND APPLICATIONS

R. A. Marcus

The activated-complex theory of chemical reactions has proved to be very useful in interpreting rate data on a wide variety of chemical reactions. The topics so treated include preexponential factors of bimolecular gas-phase reactions, preexponential factors at high pressures of unimolecular reactions,

TECHNIQUES OF CHEMISTRY, VOL. 6, PT. 1
Edited by E. S. Lewis John Wiley & Sons, Publishers, Copyright 1974

salt and polar solvent effects on bimolecular-reaction rates, and recombination rates of radicals under certain conditions. In conjunction with additional concepts, the theory has also found extensive use in such subjects as pressure effects on unimolecular reactions (so-called RRKM theory), chemical activation, and electron-transfer reactions both in solution and at electrodes.

In the present chapter the assumptions and several derivations of the theory are considered. Some of the recent tests of activated-complex theory that are based on the numerical solution of the dynamical equations of motion of the reactants are summarized. Topics such as the "free-energy-maximization criterion" for the position of the activated complex are also considered. Several of the applications of activated-complex theory are treated, and some dynamical extensions of it are noted.

Some of the work described in the present chapter is drawn from the writer's published studies, but the material in Sections 3 and 5 on an ensemble derivation for reactions in solution and on a basis for the usual free-energy-maximization criterion for location of the activated complex is drawn from unpublished work.

1 ASSUMPTIONS AND DERIVATION

Assumptions

In typical applications of activated-complex theory to a system, attention is focused on one or more molecules that may be in the process of reacting. The influence of any surrounding molecules or ions in the liquid or gas is frequently also included in the treatment, via solvation terms. In a system having N coordinates, say, one attempts to define a set of configurations occupying $N - 1$ dimensions. This set, termed a *hypersurface*, separates two parts of the space and is chosen (as much as possible) so that once the system has crossed this hypersurface, only the products can result. All the configurations belonging to the hypersurface are called the *activated complex*.

To demonstrate what is involved in the definition of this hypersurface in a little more detail, we consider an example of a reaction

$$AB + C \rightarrow A + BC \tag{2.1}$$

in which all three particles lie along a straight line. The number of coordinates N needed to describe the relative distances is two. They can be chosen to be the AB distance and the distance between C and the center of mass of AB. The curves of constant potential energy are indicated on the usual skewed plot of Fig. 2.1, where the coordinates are mass-weighted values of the above two coordinates, as discussed later.

A single point on this plot represents the values of the two coordinates,

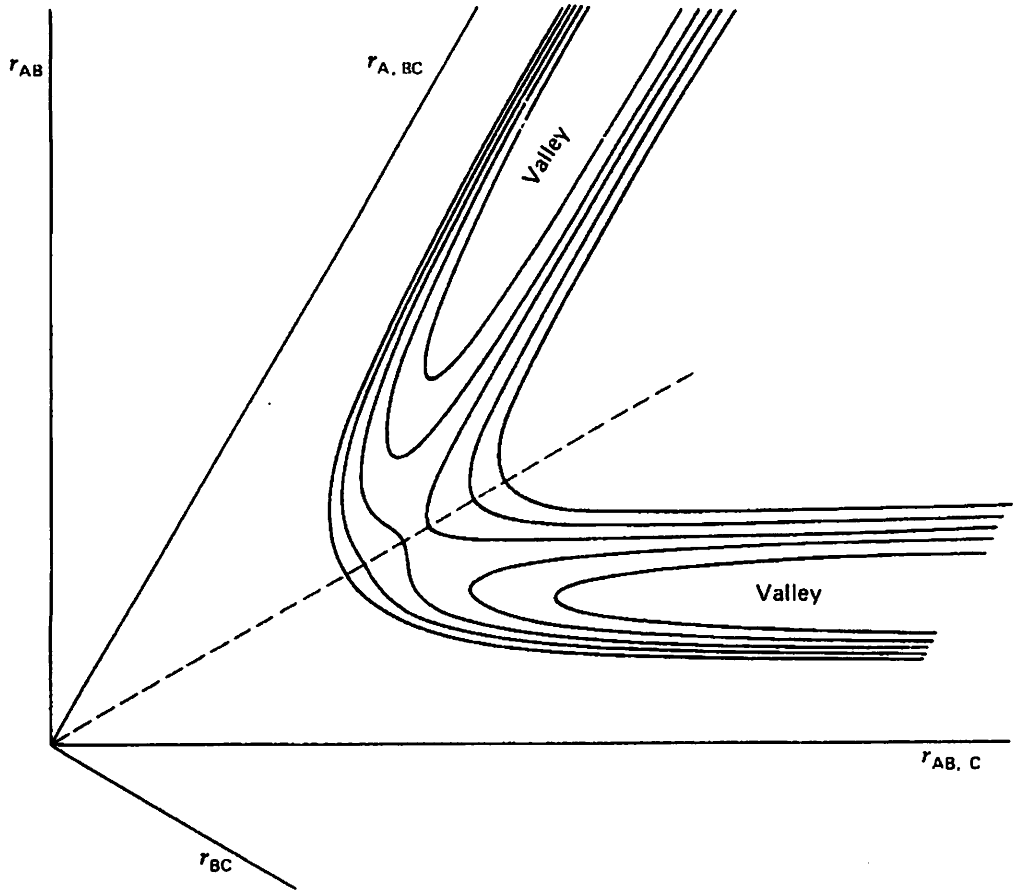

Fig. 2.1 Potential energy contours for reaction (2.1), plotted as a function of mass-weighted coordinates r_{AB} and $r_{AB,C}$ (cf. eq. 2.14). The dotted line denotes the activated complex.

and the motion of that point represents the dynamical behavior of the system. Stable configurations of reactants are in the valley in the lower right-hand valley of the figure, and those of the products lie in the upper left-hand valley. The configurations that constitute the activated complex occupy $N - 1$ dimensions (i.e., one dimension on the figure) and are represented by the dotted line in the figure. The dotted line is seen to separate the reactants' region from the products' one, and the motion away from the dotted line is downhill, on either side of the line.

The assumptions of activated-complex theory are the following:

1. A set of configurations, the $(N - 1)$-dimensional hypersurface in an N-dimensional coordinate space, can be defined as having the property that a system that has crossed it has thereby reacted.
2. There is an equilibrium between reactants and systems crossing the surface in the *forward* direction. Such an equilibrium, which does *not* involve equilibrium between reactants and systems crossing in the reverse direction, has been termed a *quasi equilibrium*.

3. In a quantum-mechanical treatment it is meaningful to speak of energy levels $E_n^\ddagger$ of the activated complex.
4. When quantum-mechanical effects are important in the rate of *crossing* of the surface (e.g., in tunneling), one *usually* assumes that the motion across the surface can be treated as a rectilinear motion and the relevant quantum mechanics for rectilinear tunneling can be applied.

Derivation

With these assumptions one can derive the customary activated-complex-theory expression as follows [1]: In activated-complex theory one first calculates a probability density for finding the system in a given quantum state n and per unit length along the direction perpendicular to the $(N - 1)$-dimensional hypersurface of configurations of the activated complex.* One then multiplies the above by the appropriate velocity and sums over all quantum states n of the activated complex. We first derive an expression for the rate constant of a gas reaction in a given volume V and temperature T. The effect of tunneling is first neglected.

We denote by s the coordinate perpendicular to this $(N - 1)$-dimensional hypersurface and denote by p_s the corresponding momentum. The value of s on the hypersurface is denoted by $s^\ddagger$. The probability of finding the system in a phase-space-volume element $ds\, dp_s$ and at the same time finding the system in a quantum state n of the activated complex is denoted by $\rho^\ddagger\, ds\, dp_s$. The latter is equal to

$$\rho^\ddagger\, ds\, dp_s = \frac{ds\, dp_s}{h} \frac{e^{-E/kT}}{Q}, \tag{2.2}$$

since $ds\, dp_s/h$ is the number of translational quantum states in $ds\, dp_s$. Here, Q is the partition function for the reactants at a given temperature and volume. E is the total energy and can be written near $s^\ddagger$ as

$$E = E_n(s) + \left(\frac{p_s^2}{2\mu}\right) + V_1(s), \tag{2.3}$$

where $E_n(s)$ is the energy of all degrees of freedom of the system on a hypersurface at any s (other than the s-coordinate), $p_s^2/2\mu$ is the kinetic energy along the reaction coordinate at that s, μ is the effective mass for motion along that coordinate, and $V_1(s)$ is the minimum potential energy on the hypersurface at this s. To discuss the crossing of the hypersurface at $s = s^\ddagger$, the $E_n(s)$ and $V_1(s)$ will be replaced by their values $E_n^\ddagger$ and $V_1^\ddagger$ at $s^\ddagger$, and $p_s^{\ddagger 2}/2\mu$ will indicate the value of the s-kinetic energy at $s^\ddagger$.

---

* For a system with N degrees of freedom, the Nth of which is the reaction coordinate, the quantum number n denotes a quantum number for each degree of freedom; that is, it denotes $(n_1, \ldots, n_{N-1})$.

When (2.2) is divided by ds, a probability per unit length is obtained, and when this result is multiplied by $\dot{s}$, the velocity along the reaction coordinate, the contribution of the specified quantum states to the reaction rate is calculated. Upon integration over all values of p_s in the positive direction—that is, from 0 to ∞—and summation over all quantum states n of the activated complex, an expression for the rate constant of the reaction k_r is then obtained:

$$k_r = \sum_n \int_0^\infty \frac{\dot{s}\, dp_s}{hQ} \exp\left[\frac{-(E_n^\ddagger + (p_s^2/2\mu) + V_1^\ddagger)}{kT}\right]. \tag{2.4}$$

Since $\dot{s}$ equals p_s/μ, $\dot{s}\, dp_s$ equals $d(p_s^2/2\mu)$ and integration of (2.4) then leads to

$$k_r = \frac{kT}{h}\frac{Q^\ddagger}{Q} e^{-V_1^\ddagger/kT} \equiv \frac{kT}{h} e^{-\Delta A^\ddagger/kT}. \tag{2.5}$$

$\Delta A^\ddagger$ is the (Helmholtz) free energy of activation and $Q^\ddagger$ is the partition function of all degrees of freedom of the activated complex apart from that of the s-motion:

$$Q^\ddagger = \sum_n \exp\left(\frac{-E_n^\ddagger}{kT}\right), \qquad \Delta A^\ddagger = -kT \ln \frac{Q^\ddagger}{Q} + V_1^\ddagger. \tag{2.6}$$

The activation energy E_a of the reaction readily follows from (2.5) by differentiating $\ln k_r$ with respect to $1/kT$:

$$E_a = \frac{-\partial \ln k_r}{\partial(1/kT)}. \tag{2.7}$$

Insertion of (2.5) into (2.7) yields terms $-\partial \ln Q^\ddagger/\partial(1/kT)$ and $-\partial \ln Q/\partial(1/kT)$, denoted by $\langle E_n^\ddagger \rangle$ and $\langle E_n \rangle$, which are the average energies of the activated complex, apart from that of the s-motion, and of the reactants, respectively. The kT term in the preexponential factor of (2.5) contributes another kT to the activation energy. Thus,

$$E_a = kT + V_1^\ddagger + \langle E_n^\ddagger \rangle - \langle E_n \rangle \qquad \text{(arbitrary } T\text{)}. \tag{2.8}$$

When the temperature is sufficiently low that all species are essentially in their lowest quantum state of energy E_0 (reactants) or $E_0^\ddagger + V_1^\ddagger$ (activated complex), $\langle E_n^\ddagger \rangle$ and $\langle E_n \rangle$ become the energies in the lowest states of the activated complex and reactants, respectively. One then obtains

$$E_a = V_1^\ddagger + E_0^\ddagger - E_0 \qquad (T = 0°\mathrm{K}). \tag{2.9}$$

Extension of Concepts

In the previous section we were mainly concerned with the crossing of a hypersurface at $s = s^\ddagger$, an $s^\ddagger$ that was independent of n, the quantum state of activated complex. To treat systems where $s^{\ddagger}$ depends on n or where quantum-mechanical tunneling occurs through a wide barrier or where a free-energy criterion is considered (see Section 5), it is desirable to extend some of the concepts of the previous section.

The two-dimensional system in Fig. 2.1, will serve for purposes of illustration. One may imagine that curvilinear reaction-coordinate curves have been introduced (curves on which the *vibrational coordinate* is constant). One example of such curves is illustrated by a family of curves in Fig. 2.2, of which L, L', and L'' are members. Hypersurfaces (one-dimensional in the present figure) of constant s are illustrated by the dotted lines.

Curve L itself passes along the floor of the valley of the reactants in the lower right of Fig. 2.2, over the saddle-point, and then down to the floor of the products in the upper left of Fig. 2.2 (L is thereby the curve of lowest potential energy V leading from reactants to products). Along L, V has a

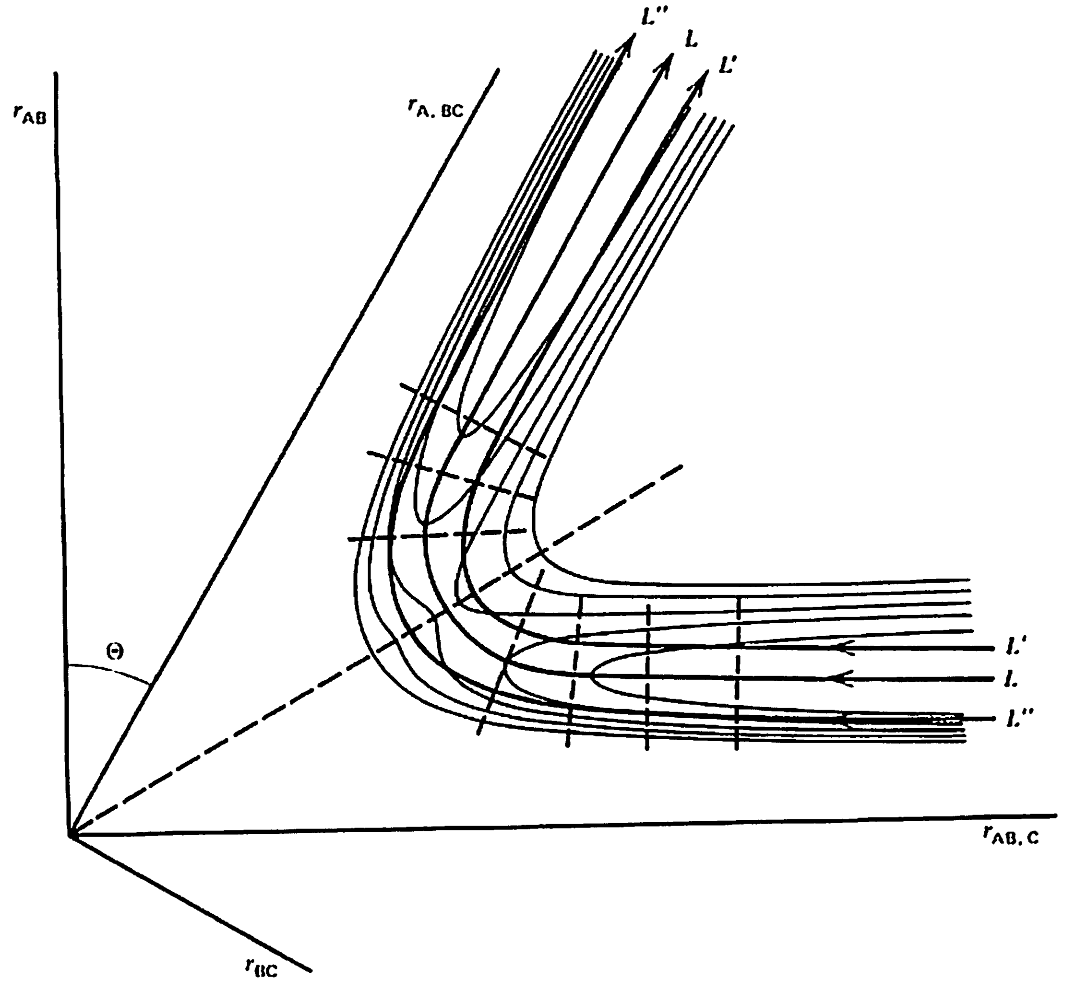

Fig. 2.2 Illustration of hypersurfaces at different values of s (the dotted lines normal to L-curves) and of reaction coordinate curves L, L', L'' differing in value of the vibrational coordinate (r in Fig. 2.6).

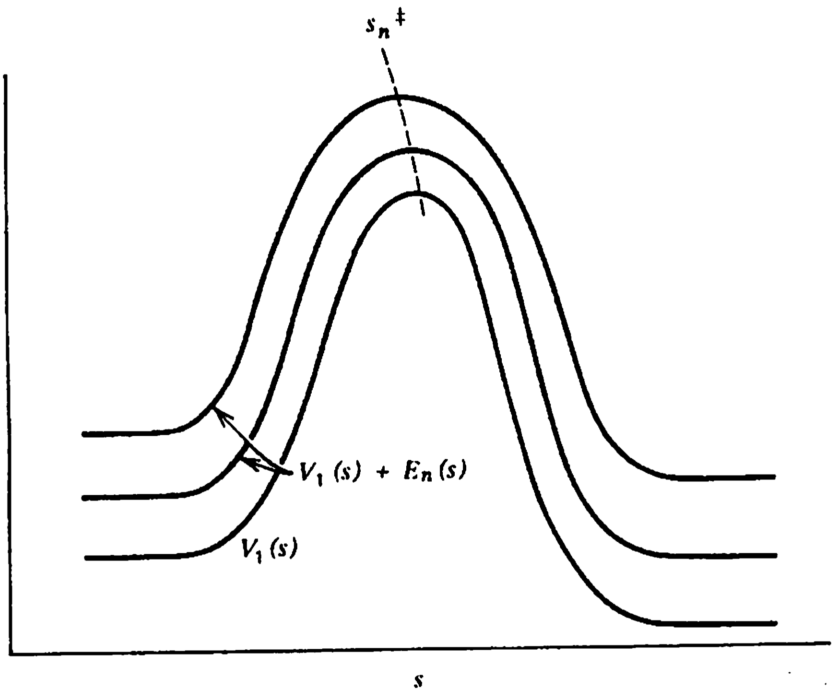

Fig. 2.3 Plot of effective potential energy $V_1(s) + E_n(s)$, for two states n, along the reaction coordinate, and plot of $V_1(s)$

value $V_1(s)$, the minimum value of V on any hypersurface at a given s [cf. (2.3)].

Classically the point representing the reacting system would oscillate in the reactants' valley and at the same time move from this valley, in which the reactants are far apart, over the dotted line occupying a saddle-point region, and into a valley in which the products are far apart.

If we now use (2.3) for all values of s (a point commented on later), $E_n(s)$ is the energy, kinetic plus potential, the potential measured relative to that on L, for motion on the hypersurface. In this example of Figs. 2.1 and 2.2, $E_n(s)$ is the usual vibrational energy. A plot of the potential energy V along curve L, that is, $V_1(s)$—for a surface somewhat less symmetrical than that given in Figs. 2.1 and 2.2—is given in Fig. 2.3, together with a plot [2] of $E_n(s) + V_1(s)$ for some n.

Activated Complexes Whose Position Is State-Dependent

Apart from a quantum-mechanical treatment of the s-motion, (2.5)–(2.9) do not include the possibility, which is sometimes important, that $s^‡$, the position of the $(N - 1)$-dimensional hypersurface, may depend upon the quantum state n of the activated complex [2, 3]. Specifically, the maximum of $E_n(s) + V_1(s)$ can depend on n as in Fig. 2.3. A simple example of this dependence occurs when part of the barrier to a bimolecular reaction arises from a centrifugal potential of the colliding molecules [4]. The orbital angular-momentum quantum number l then contributes to n.

For the case where $s^‡$ depends on n, and so is denoted by $s_n^‡$, (2.4) is still valid, except that $E_n^‡$ and $V_1^‡$ are the values at the maximum of $E_n(s) + V_1(s)$

(i.e., at $s = s_n^\ddagger$). For each n, the integration of (2.4) over p_s is performed at that $s_n^\ddagger$. As before, $\dot{s}\, dp_s$ equals $d(p_s^2/2\mu)$ and one ultimately obtains

$$k_r = \frac{(kT/h)Q_{\mathrm{eff}}^\ddagger}{Q} \tag{2.10}$$

where

$$Q_{\mathrm{eff}}^\ddagger = \sum_n \exp\left[\frac{-(E_n^\ddagger + V_1^\ddagger)}{kT}\right] \tag{2.11}$$

and

$$E_n^\ddagger + V_1^\ddagger \equiv E_n^\ddagger(s_n^\ddagger) + V_1^\ddagger(s_n^\ddagger). \tag{2.12}$$

Equations (2.10)–(2.12) include as a special case the treatment of many years ago of recombination of free radicals [4, 5], in which centrifugal potential and van der Waals' attraction were assumed to dominate the interactions. Steric effects were omitted in the latter. They are normally small in the specific instance of free-radical recombinations but can be present in other systems. They contribute to $E_n(s)$ and so are automatically included in (2.11).

Tunneling Contribution

In discussing the classical s-motion across a hypersurface in the interval $(s^\ddagger, s^\ddagger + ds)$, the s-motion can be treated as rectilinear. In a quantum-mechanical treatment of the s-motion, a rectilinear coordinate can be used for sufficiently small degrees of tunneling, since only regions close to the usual saddle-point in the potential-energy surface in Fig. 2.1 would then contribute to k_r. With larger amounts of tunneling, the curvilinear nature of the s-motion should be considered, as one sees from Fig. 2.2.

It is useful to recall a definition of the skewed axes and of an effective mass μ, by examining the definition of the coordinates, for example, for the reaction

$$\mathrm{AB} + \mathrm{C} \rightarrow \mathrm{A} + \mathrm{BC}. \tag{2.13}$$

We illustrate the origin of this μ by considering for simplicity the case of A, B, and C as being on a line, but the same definition of μ applies in the actual full three-dimensional system [6]. Of the resulting three coordinates, the position of the center of mass of the three atoms can be chosen as one coordinate. It can be omitted from the present discussion of rate constants, since it does not affect the interactions and, hence, does not affect the reaction rate. The two remaining coordinates can be taken to be the AB distance, R_{AB}, and the distance between C and the center of mass of AB, $R_{\mathrm{AB,C}}$. With such a choice the kinetic energy for these two degrees of freedom contains no cross-terms [4].

One further frequently introduces mass-weighted coordinates [4]. Then, the motion in this two-coordinate system can be represented by a single point moving in Fig. 2.1 with a single effective mass μ [4, 6]. The new coordinates are denoted by r_{AB} and $r_{AB,C}$, respectively. μ could be chosen equal to unity, affecting thereby the scaling factor in r_{AB} and $r_{AB,C}$.

When discussing the motion of the reaction *products* it is convenient to introduce mass-weighted coordinates $r_{A,BC}$ and r_{BC}, which are linear combinations of the two previously introduced coordinates and which also contain no cross terms in their kinetic energy [4]. They are indicated in Fig. 2.1.

The kinetic energy of the system thereby equals

$$T = \tfrac{1}{2}\mu(\dot{r}_{AB}{}^2 + \dot{r}^2_{AB,C}) = \tfrac{1}{2}\mu(\dot{r}_{BC}{}^2 + \dot{r}^2_{A,BC}). \tag{2.14}$$

One set of coordinates is obtained from the other set by rotation through an angle θ in Fig. 2.1, where [4]

$$\sin\theta = \left[\frac{m_A m_C}{(m_A + m_B)(m_C + m_B)}\right]^{1/2}. \tag{2.15}$$

To consider tunneling, now, it will be assumed that the motion along a reaction coordinate s can, in the activated-complex region, be separated from the remaining motions and that a rectilinear expression for the kinetic energy of the reaction coordinate s can be used. That is, curvilinearity of the s-coordinate curves is neglected in the usual treatment. After this "adiabatic separation of variables" of the internal motion at each s to obtain $E_n(s)$, one then solves the separated wave equation of the s-motion in the vicinity of the potential-energy maximum:

$$\left[-\frac{\hbar^2}{2\mu}\frac{d^2}{ds^2} + V_1(s) + E_n(s)\right]\Psi_{En}(s) = E\Psi_{En}(s). \tag{2.16}$$

The effective barrier for the tunneling, $V_1(s) + E_n(s)$, is depicted for some n in Fig. 2.4.

Since the tunneling is through a $V_1(s) + E_n(s)$ barrier, rather than through the $V_1(s)$ barrier along L, the system actually tunnels along the entire family of L curves in Fig. 2.2. The contribution from each L curve is weighted in a subtle way [by the contribution of the vibrational wave function to $E_n(s)$].

Solution of (2.16) yields the probability $\kappa(E, n)$ that the system crosses the activated-complex region. The energy for the remaining degrees of freedom has some value $E_n^\ddagger$ in the activated-complex region. The arguments leading from (2.3) to (2.5) can again be used, in a somewhat modified manner, but now including tunneling.

The probability of finding the system in a phase-space-volume element $ds\, dp_s$ at some specified s near to, but to the left of, point a in Fig. 2.4, and at the same time of finding the system in a quantum state n for the remaining

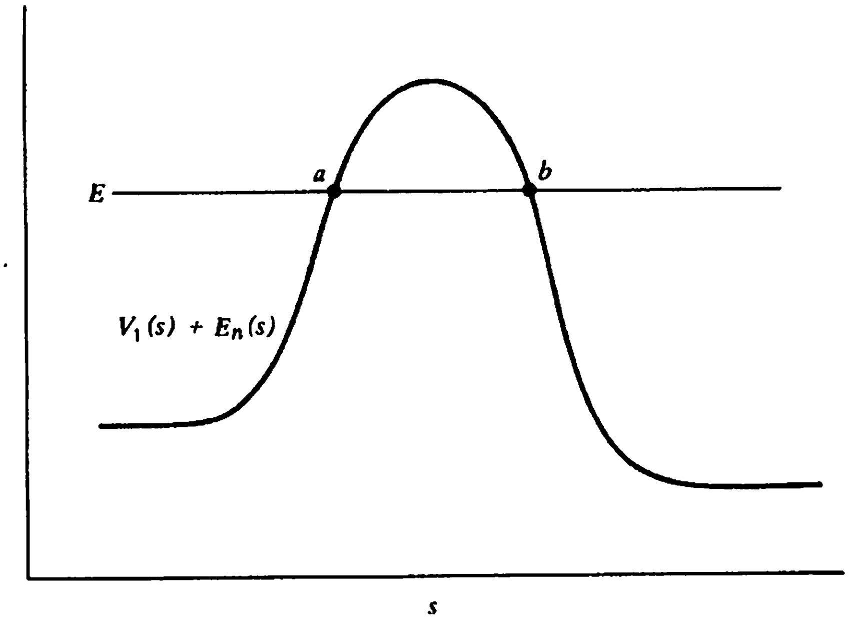

Fig. 2.4 Plot of the effective potential energy $V_1(s) + E_n(s)$ versus reaction coordinate. Points a and b are "turning-points" (i.e., points where the classical momentum p_s vanishes).

degrees of freedom, is $\rho\, ds\, dp_s$:

$$\rho\, ds\, dp_s = \frac{ds\, dp_s}{h} \frac{\exp\{-[E_n(s) + V_1(s) + (p_s^2/2\mu)]/kT\}}{Q} \qquad (s < a), \tag{2.17}$$

recalling (2.3). After dividing by ds, one obtains the probability per unit length at the given s. When this result is multiplied by $\dot{s}$, the velocity along the reaction coordinate at that s, the probability flux of systems incident on the reaction barrier is obtained. Of this incident flux, only a fraction $\kappa(E, n)$ passes into the products' region. Upon multiplying the above expression by $\kappa(E, n)$, integrating over all positive values of p_s, and summing over all quantum states n of the activated complex, an expression is obtained for the rate constant k_r:

$$k_r = \sum \int \kappa(E, n) \exp\{-[E_n(s) + V_1(s) + (p_s^2/2\mu)]/kT\} \frac{\dot{s}\, dp_s}{hQ}. \tag{2.18}$$

Since $E_n(s) + V_1(s) + (p_s^2/2\mu)$ is E and $\dot{s}\, dp_s$ is dE, one obtains [3]

$$k_r = \frac{kT}{h} \int_E \kappa(E, n) e^{-E/kT} \frac{dE/kT}{Q}. \tag{2.19}$$

When the dependence of $E_n(s)$ on s in the vicinity of $s^\ddagger$ is negligible, and written as $E_n^\ddagger$, then $\kappa(E, n)$ depends on E and n only via $E - E_n^\ddagger$. Denoting the latter by $\epsilon + V_1^\ddagger$, ϵ equals $E - E_n^\ddagger - V_1^\ddagger$ and so is the "translational energy" at $s^{\ddagger}$. Equation (2.19) can be written as

$$k_r = \frac{kT}{h}\int \kappa(\epsilon)e^{-\epsilon/kT}\frac{d\epsilon}{kT}\frac{Q^{\ddagger}}{Q}\exp\left(\frac{-V_1^{\ddagger}}{kT}\right). \tag{2.20}$$

When there is no tunneling, $\kappa(\epsilon)$ in (2.20) is zero when ϵ is negative and equals unity when ϵ is positive. In this case the integral over ϵ becomes unity and (2.20) reduces to (2.5). Similarly, (2.19) can be shown to reduce to (2.10) in the absence of tunneling.

A semiclassical value for $\kappa(\epsilon)$ in (2.20), when $\epsilon < 0$, is [3]

$$\kappa(\epsilon) = \frac{1}{1+\alpha^2} \tag{2.21}$$

where

$$\alpha = \exp\left(\int_a^b |p_s|\frac{ds}{\hbar}\right). \tag{2.22}$$

a and b are defined in Fig. 2.4, and

$$p_s = \pm\{2\mu[E - V_1(s) - E_n^{\ddagger}]\}^{1/2}. \tag{2.23}$$

A related expression can be written for $\kappa(\epsilon)$ for $\epsilon > 0$ [3]. As an example of (2.21)–(2.23), one may consider the case where $V_1(s)$, the potential energy along curve L in Fig. 2.3, is a parabola, $V_1^{\ddagger} - \frac{1}{2}k(s - s^{\ddagger})^2$. The integral in (2.22) is given by

$$\int_a^b |p_s|\frac{ds}{\hbar} = \int_a^b |\{2\mu[-\epsilon - \tfrac{1}{2}k(s - s^{\ddagger})^2]\}^{1/2}|\frac{ds}{\hbar}. \tag{2.24}$$

The points a and b are those where the integrand vanishes. The integral is a standard one and equals $(-\pi\epsilon)/h\nu$, where ν is the "frequency" of s-motion, $(1/2\pi)\sqrt{k/\mu}$. ϵ is negative in the tunneling region.

This special case of (2.21)–(2.23), where $V_1(s)$ is a parabolic barrier, was treated by Bell by other methods [7], but curiously enough (2.20)–(2.23) have rarely been used in the tunneling literature. Instead the $V_1(s)$ has been fitted to an Eckart potential [1] or numerical solutions have been employed.

One can also derive the curvilinear counterpart of (2.20)–(2.23), and we refer the reader to the relevant literature [2, 8].

2 BASIS OF ACTIVATED-COMPLEX THEORY

The possible dynamical basis of activated-complex theory is a topic of considerable interest and not yet fully understood. In some cases the derivation of activated-complex theory from first principles is fairly clear, and we shall discuss them. In all the cases below it will be assumed that the distribution of the reactants themselves among quantum states is a Boltzmann distribution. Calculations that have been made of the deviation from Boltzmann population of reactants due to reaction suggest such effects to be relatively small [9].

Highly Exothermic Reactions

When a highly exothermic reaction has a negligible activation energy barrier and when there is a long-range attractive interaction, the activated complex sometimes occurs at a relatively large distance of approach R of the two reactants. In this case, the dynamical problem becomes simply a two-body problem and one need consider only the long-range attractive contribution to the potential energy.

As usual for such two-body problems having a potential $V(R)$ that depends only upon R, one introduces polar coordinates, "separates variables," and finds that the radial motion obeys the equation

$$\frac{p_R{}^2}{2\mu} + V_{\text{eff}}(R) + E_n = E, \tag{2.25}$$

where p_R is the radial momentum $\mu\dot{R}$, E_n is the energy of the other coordinates, and $V_{\text{eff}}(R)$ is an effective potential energy:

$$V_{\text{eff}}(R) = V(R) + \frac{l(l+1)\hbar^2}{2\mu R^2}. \tag{2.26}$$

The last term in (2.26) is the usual centrifugal potential, l being the orbital angular momentum. The other degrees of freedom of the reactants remain, in the present example, in the same quantum state from the beginning of the collision to (at least) the point where the system passes the activated-complex hypersurface and have an energy E_n. By an argument the same as that leading to (2.12), the exact dynamics lead to that equation, but with $E_n(s_n^\ddagger)$ now replaced by $E_n + V_{\text{eff}}(R_n^\ddagger)$, where $R_n^\ddagger$ is the R for which (2.25) is a maximum and where l is one of the quantum numbers contributing to n.

The potential energy surface for a low-activation-energy, highly exothermic reaction is sketched in Fig. 2.5. Activated-complex theory for this system is obeyed, provided a system that has crossed the dotted line is not reflected back to reform reactants, upon striking the bent region of the "reaction channel" in Fig. 2.5. An example appears later in [23].

Highly Endothermic Reaction

If we consider the reverse reaction, a highly endothermic reaction, it will have the same activated complex as above and, by microscopic reversibility, will also obey activated-complex theory. During the reaction, the system in

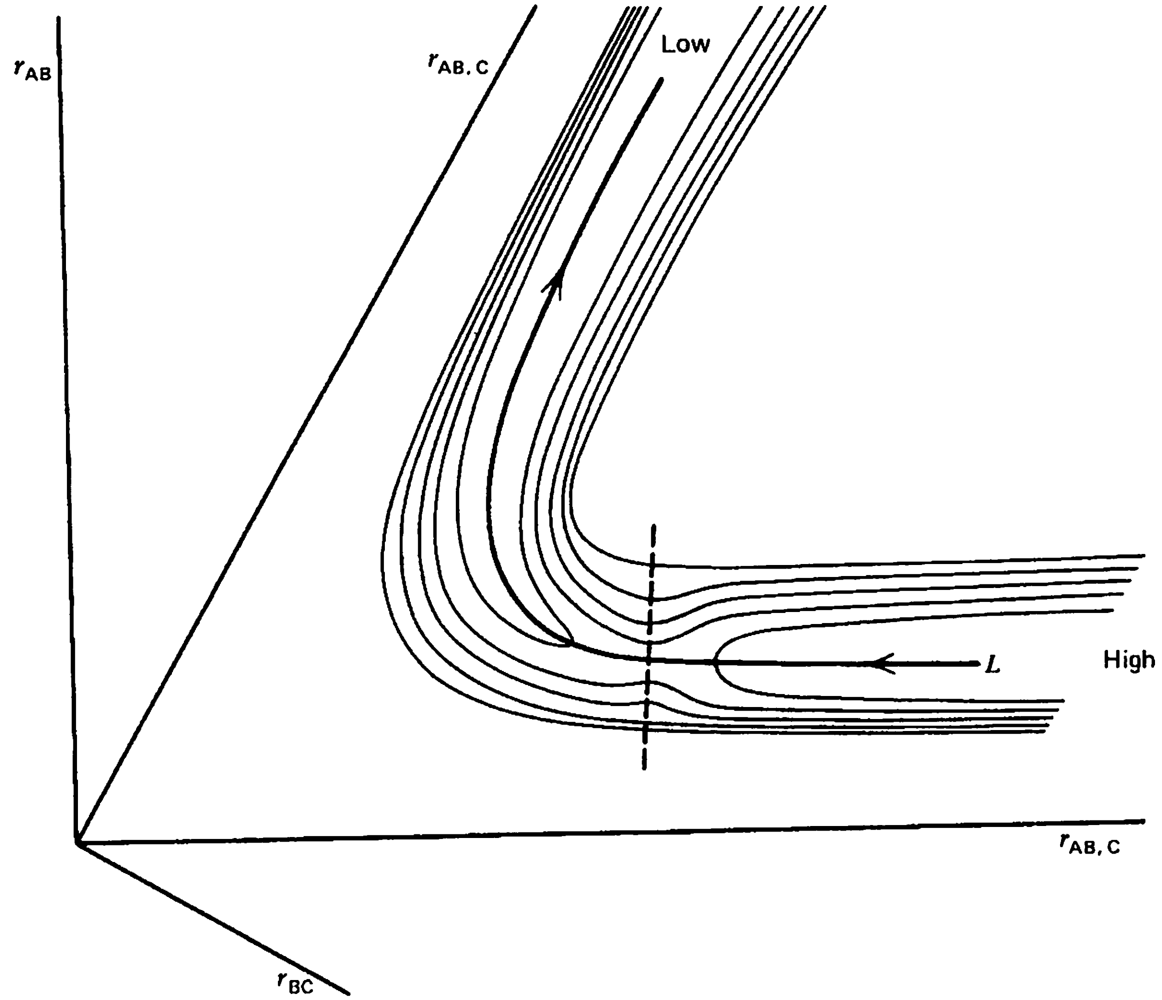

Fig. 2.5 Potential energy contours for reaction (1.1) for a highly exothermic reaction, with activated complex in reactant's valley (cf. Fig. 2.1).

the vicinity of the curve *L* in Fig. 2.5 proceeds from the upper portion to the lower right-hand portion. For later use, we note that it obeys activated-complex theory, even though there are now considerable changes in internal quantum states before reaching the activated complex from the left.

Statistically Vibrationally Adiabatic Reactions

We consider now a different class of reactions, those for which the dynamical basis for activated-complex theory is a more subtle one than the above. Many years ago it was suggested that if the system somehow remained in the same quantum state during motion along the reaction coordinate an activated-complex-theory equation would be obeyed [10]. Such a system could be called *adiabatic* in the quantum-mechanical sense of the term, in so far as the motions other than s are concerned. It has, for brevity, been called *vibrationally adiabatic* [11].

Apart from the rare case where the reaction coordinate is rectilinear, the detailed meaning of "remaining in the same quantum state" was not specified in this earlier period, for systems with smooth potential-energy surfaces: no way for defining such a state for all values of the reaction coordinate had been offered. (For that purpose we shall later utilize "natural collision coordinates" [11, 12]). The suggestion of this adiabaticity [10, 4] passed largely unnoticed and was subsequently "rediscovered" independently by a number of investigators, with added insights or elaborations [13–15].

We consider first, therefore, natural collision coordinates [11]. Such coordinates pass smoothly from those suited to reactants to those suited to the activated complex and to those suited to products. They are sketched for a linear collision in Fig. 2.6. In this space a curve *C* is drawn as indicated and, from any point *P*, a perpendicular to the curve is also drawn. The curve *C* need not coincide with the reaction path *L*, but it is sometimes convenient to choose it this way, as in fact we have done by using the family of *L*-curves in Fig. 2.2 as the reaction-coordinate curves.

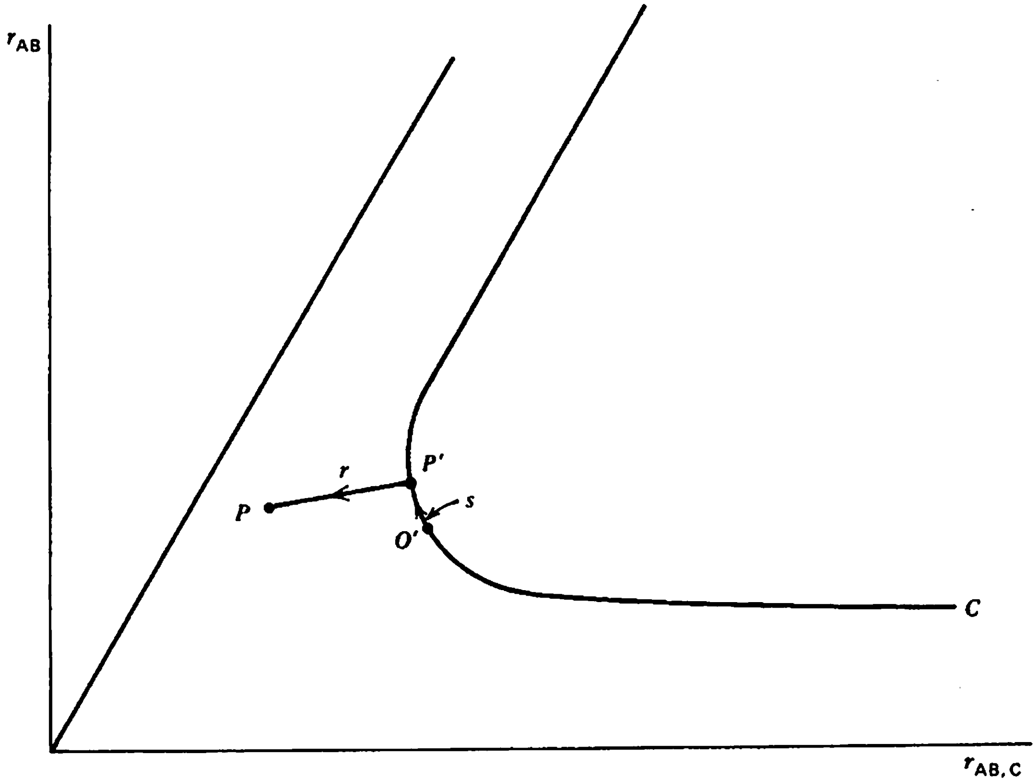

Fig. 2.6 Natural collision coordinates s and r, s being the reaction coordinate and r the vibrational coordinate (cf. Fig. 2.2).

The distance from *P* to *P*′, the foot of the perpendicular from *P* to curve *C*, is one coordinate, *r*, and is positive on one side of the curve and negative on the other. The arc length from any fixed point *O*′ on the curve to *P*′ is the second coordinate *s*. The kinetic energy of the system can be expressed in terms of the velocities, $\dot{r}$ and $\dot{s}$, and the curvature $\kappa(s)$ of curve C [11]:

$$T = \tfrac{1}{2}\mu(\dot{r}_{\mathrm{AB}}{}^2 + \dot{r}_{\mathrm{AB,C}}) = \tfrac{1}{2}\mu[(1 + \kappa r)^2\dot{s}^2 + \dot{r}^2]$$

$$= \left(\frac{1}{2\mu}\right)\left[\frac{p_s{}^2}{(1 + \kappa r)^2} + p_r{}^2\right], \quad (2.27)$$

$\kappa(s)$ is a function of s and is zero at $s = \pm\infty$. [This $\kappa(s)$ is not to be confused with the transmission probability $\kappa(E, n)$ used in a previous section and later in (2.30).] The terms p_s and p_r are the momenta corresponding to s and r, respectively:

$$p_s = \mu(1 + \kappa r)\dot{s}, \qquad p_r = \mu\dot{r} \quad (2.28)$$

The potential energy of the system $V(r, s)$ can be expressed as

$$V(r, s) = V_1(s) + V_2(r; s) \quad (2.29)$$

where $V_1(s)$ is the value of V at P' on curve C, and V_2 is the increment to go from P' to P, in Fig. 2.6.

Coordinate r is a vibrational coordinate throughout the collision, as one can see from Fig. 2.6. For reaction (1.1), it is the vibrational coordinate of the reactant AB at large negative values of s, the vibrational coordinate of the product BC at large positive values of s, and a symmetric stretching vibrational coordinate of the activated complex in the vicinity of $s = s^\ddagger$. The coordinate s is, apart from an additive constant, seen to be the distance between the products at large negative values of s, the distance between the products at large positive values of s, and the usual asymmetric stretching-vibration reaction coordinate near $s = s^\ddagger$. Thus, s is the reaction coordinate, defined now not only in the vicinity of the activated complex, the reactants' and the products' region, but throughout the reaction. We consider now the meaning of "remaining in the same vibrational quantum state during the collision."

When the r- and s-motions are independent—for example, in the region of large negative or large positive s—the system remains in the same vibrational quantum state regardless of how large $\dot{s}$, the s-component of velocity, is. However, the system will tend to be excited or de-excited vibrationally when $\dot{s}$ is large in the region near the bent part of curve L in Fig. 2.1. Thus, provided $\dot{s}$ is small in that region, the system can be characterized as vibrationally adiabatic by writing the wave function as

$$\psi(r, s) \cong \psi_n(r; s)\psi_{En}(s), \quad (2.30)$$

where $\psi_n(r; s)$ is the vibrational wave function, which depends mainly on r but also parametrically on s. The force constant, for example, varies with s

at intermediate s values, and so, $\psi_n(r; s)$ varies with s. $\psi_{En}(s)$ is the wave function describing the motion along the reaction coordinate.

Wave functions analogous to that in (2.28) are very common in other problems. For example, in the Born-Oppenheimer approximation used to separate electronic and nuclear motions, ψ_n would be the electronic wave function (r would then denote the electronic coordinates), and $\psi_{En}(s)$ would be the nuclear wave function (s would denote the atomic positions). The adiabaticity would be one of *electronic* adiabaticity.

Using $\psi_n(r; s)$ as an approximate wave function, the vibrational energy levels of the system $E_n(s)$ can be calculated as a function of s, and when added to the potential-energy term $V_1(s)$, they constitute an effective potential energy for a motion along the reaction coordinate. Schematic plots of this effective potential energy were given in Fig. 2.3.

Using the wave function in (2.28) as a zero-order approximation, one can then calculate transition probabilities to other vibrational states of the system, quantum mechanically or classically, as a result of the reaction [11, 13]. However, we shall examine instead how one may derive activated-complex theory from dynamics when the vibrationally adiabatic approximation is made.

A formal expression for the rate constant k_r, given by (2.32), is first derived and *then* the vibrationally adiabatic approximation is introduced to yield (2.10)–(2.12).

The probability of finding the reactants in some initial state n and in a phase-space region $ds\, dp_s$ in the reactant's region (large negative s) is

$$\rho\, ds\, dp_s = \frac{ds\, dp_s}{h} \frac{\exp(-E/kT)}{Q}, \tag{2.31}$$

where E is total energy of the reacting molecule or molecules. Dividing by ds and multiplying by $\dot{s}$ and by a transmission coefficient $\kappa(E, n)$ (to be evaluated later) for reaching the products from this initial state, integrating over all E, and summing over all n, one obtains

$$k_r = \frac{kT}{h} \sum_n \int_E \kappa(E, n) \exp\left(\frac{-E}{kT}\right) \frac{d(E/kT)}{Q}, \tag{2.32}$$

since $\dot{s}\, dp_s$ equals dE, as before.

Expression (2.32) is a formal one until a prescription is given for calculating $\kappa(E, n)$, and as yet the vibrationally adiabatic approximation has not been introduced. In this assumption (2.30) for ψ is valid for all s. Neglecting curvilinear effects and, for the moment, treating the s-motion classically, the total energy E can be written as

$$E = E_n(s) + V_1(s) + \frac{p_s^2}{2\mu}, \tag{2.33}$$

with n independent of s when one assumes vibrational abiabaticity. $\kappa(E, n)$ is unity if the $p_s^2/2\mu$ given by (2.33) is positive for all s. Otherwise, $\kappa(E, n)$ is zero. Integration of (2.32) then yields (2.10)–(2.12). These equations reduce to (2.4)–(2.6) when the dependence of $s^\ddagger$ on n can be neglected. Inclusion of tunneling again yields (2.19) and (2.20) instead of (2.4)–(2.6). Inclusion of curvilinear effects introduces, among other things, a position-dependent coefficient of p_s^2, namely, $(1 + \kappa r)^{-2}$ in (2.33) [11] and a treatment of curvilinear effects has been given elsewhere [3, 14].

For a vibrationally adiabatic system the energy levels $E_n(s)$, and hence $E_n(s^\ddagger)$, entered quite naturally, because of the wave function (2.30). However, the coupling present between the s and other motions would be expected to lead at least to a distribution of the n at $s^\ddagger$ about the adiabatic value (statistical adiabaticity) and, at stronger coupling, to distribution about some other value [16]. The statistical adiabaticity would be expected intuitively to yield a k_r approximately the same as that given by a vibrationally adiabatic system.

Again, when one considers three-dimensional collisions, the rotational motion of the reactants, coupled with the orbital motion and to some extent with the vibrational motion, evolves into the bending vibrations of the activated complex. The orbital motion, coupled with the rotational motion, evolves into the overall rotation of the activated complex. Adiabaticity for such degrees of freedom is too restrictive, and statistical adiabaticity or even a more random (Boltzmann-like) statistical distribution [17] among levels $E_n^\ddagger(s^\ddagger)$ might be more appropriate. Both can still lead, approximately, to the activated-complex-theory expression.

Summary

In summary, there are a number of dynamical situations in which activated-complex theory will result, in the first approximation. Because of the wide range of such possibilities, ranging from highly vibrationally adiabatic to highly vibrationally nonadiabatic, and to statistical, one cannot equate activated-complex theory with any of these alone, although each may sometimes provide useful insight into the dynamics in the system.

One can suppose that a necessary condition for validity of activated-complex theory is that (a) the states $E_n(s^\ddagger)$ be reasonably accessible from the initial states, either by a vibrationally adiabatic or statistically adiabatic evolution from the initial states as the system moves along the coordinate s or by a statistical redistribution of relatively closely spaced states as a result of strong coupling; and that (b) systems passing through the activated-complex region should not subsequently be reflected back, in their motion along s, to reform reactants.

The strength of activated-complex theory for calculating rate constants is its broad base, indicated above. By the same token its weakness would be its inability to calculate the now frequently measurable more dynamical properties, such as distribution of final states of products.

3 ACTIVATED-COMPLEX THEORY FOR SOLUTIONS

The derivation in Section 1 referred to a system of a given volume and temperature, whereas in solution the reaction proceeds at a given pressure P and temperature T. To treat the latter, one should use the appropriate ensemble. The probability of finding the system in some quantum state n of energy E_n and with some volume V in such an ensemble $\rho(\mathbf{n}, V)$ is [18]

$$\rho(\mathbf{n}, v) = C \exp\left(-\frac{[E_{\mathbf{n}}(V) + PV]}{kT}\right) \tag{2.34}$$

where C is a normalizing factor, related to the Gibbs free energy G of the system

$$C = e^{-G/kT} = \sum_{\mathbf{n},V} \exp\left(-\frac{[E_{\mathbf{n}}(V) - PV]}{kT}\right) \tag{2.35}$$

The summation over V is actually an integration, since V is a continuous variable. The energy levels $E_{\mathbf{n}}$ can depend on V.

In the present case, as in Sections 1 and 2, one considers quantum states for the (translational) s-motion and the internal motion. The number of quantum states such that s and p_s are in the phase-space-volume element $ds\, dp_s$ and such that the system is in a particular quantum state n for the remaining degrees of freedom, is $ds\, dp_s/h$. The probability of finding the system in these states and in a volume $V^{\ddagger}$ is $\rho\, ds\, dp_s$,

$$\rho\, ds\, dp_s = \frac{ds\, dp_s}{h} \exp\left[\frac{G - E_n(s, V^{\ddagger}) - (p_s^2/2\mu) - V_1(s, V^{\ddagger}) - PV^{\ddagger}}{kT}\right]. \tag{2.36}$$

The $E_n(V)$ in (2.34) has been written as $E_n(s, V^{\ddagger}) + (p_s^2/2\mu) + V_1(s, V^{\ddagger})$. The probability per unit length along s is obtained, as before by dividing by ds, and the contribution to the reactive flux is obtained by then multiplying by $\dot{s}$, integrating over p_s for motion in the forward direction and summing over n and $V^{\ddagger}$. As before, tunneling is first neglected. The maximum of $E_n(s, V^{\ddagger}) + V_1(s, V^{\ddagger})$ along s occurs at some $s_n^{\ddagger}$, which can now depend on $V^{\ddagger}$, and defines the position of the activated complex. For each n, the integration over p_s is performed at that $s_n^{\ddagger}$. As before, $\dot{s}\, dp_s$ equals $d(p_s^2/2\mu)$ and the net result for the rate constant k_r is

$$k_r = \frac{kT}{h} \exp\left(-\frac{\Delta G^{\ddagger}}{kT}\right) \tag{2.37}$$

where $\Delta G^{\ddagger}$ is $G^{\ddagger} - G$, G is given by (2.35), and

$$\exp\left(-\frac{G^{\ddagger}}{kT}\right) = \sum_{n,V^{\ddagger}} \exp\left(-\frac{[E_n(s_n^{\ddagger}, V^{\ddagger}) + V_1(s_n^{\ddagger}, V^{\ddagger}) + PV^{\ddagger}]}{kT}\right). \quad (2.38)$$

$G^{\ddagger}$ is the Gibbs free energy of the activated complex. When $s_n^{\ddagger}$ does not depend on n significantly, $G^{\ddagger}$ is the Gibbs free energy of a system on a hypersurface at $s = s^{\ddagger}$, and then

$$\exp\left(-\frac{G^{\ddagger}}{kT}\right) = \sum_{V^{\ddagger}} \exp\left(-\frac{V_1(s^{\ddagger}, V^{\ddagger})}{kT}\right) \sum_{n} \exp\left(-\frac{[E_n(s^{\ddagger}, V^{\ddagger}) + PV^{\ddagger}]}{kT}\right). \quad (2.39)$$

Equations (2.37)–(2.38) are the analogues of (2.10)–(2.11), and (2.37) and (2.39) are the analogues of (2.5)–(2.6). As before, tunneling could readily be included and one would obtain the analogue of (2.19)–(2.20).

4 TRAJECTORY TESTS OF ACTIVATED-COMPLEX THEORY

There have been many calculations of classical trajectory studies for various reaction systems, both bimolecular and unimolecular, primarily for purposes of comparison with data on molecular beam experiments and on infrared chemiluminescence [19]. Several such calculations have also been performed for testing activated-complex theory and are considered in the present section. We consider bimolecular reactions first.

Comparisons between the numerical results of classical trajectories and classical mechanical activated-complex theory have been made for both one-dimensional (collinear) systems and full three-dimensional systems. Both bimolecular and unimolecular reactions have been treated. In the case of quantum-mechanical calculations, however, the comparisons thus far are few and restricted to linear collisions. In the next few years one may expect three-dimensional numerical quantum-mechanical results to become available and answer some important questions.

Full three-dimensional numerical classical trajectory calculations have been made for the $H + H_2 \rightarrow H_2 + H$ reaction [20]. The data have been reported in the form of total reaction cross sections as a function of initial relative velocity of reactants, initial rotational state, and initial vibrational state. The first comparison of purely classical trajectory results with *purely classical* activated-complex theory was made several years ago [21]. Trajectory data were available, at that time, for only the lowest initial vibrational state of H_2, rather than for all classical states, and so adiabaticity was assumed, to perform the calculation. Microcanonical activated-complex theory [21], which is actually the Laplace transform [21, 22], of the usual activated-complex theory, was used, the former referring to systems at a given total energy E and the latter to systems at a given temperature. In the canonical or constant-temperature activated-complex theory one calculates rate constants, while in the microcanonical or constant-energy activated-complex theory one calculates energy-averaged cross sections.

The resulting comparison is given for the $H + H_2$ reaction in Table 2.1, where σ is the reaction cross section, p is the initial momentum, and the summation is really an integral over all initial states (for a given initial vibrational state) consistent with the given total energy E. The energies are those of interest for the thermal reaction (300–1000°K). The agreement between numerical results and activated-complex theory is good, surprisingly so.

Table 2.1 Comparison of Numerical Results with Microcanonical Activated-Complex Theory [21]

E (*total*) (kcal/mole)	$\sum p^2\sigma/\pi\hbar^2$ (*numerical*)	$\sum p^2\sigma/\pi\hbar^2$ (*activated complex*)
15.5	9.6	7
17.0	24.5	22
18.5	55	50

A comparison of numerical trajectory and a microcanonical activated-complex theory result for the one-dimensional (collinear) form of the reaction $H + H_2 \rightarrow H_2 + H$ has also been made [23]. The agreement between trajectory-calculated and activated-complex-theory-calculated results was good.

The linear collision $H + HBr \rightarrow Br + H_2$ reaction, a low-activation-energy and fairly exothermic system, has also been investigated at energies corresponding to reaction temperatures of the order of, or below, 500°K [23]. There was good agreement between trajectory and activated-complex theory results. At appreciably higher energies studied in the $Br + H_2 \rightarrow H + HBr$ reaction, the activated-complex-theory-calculated reaction probability exceeded the numerical trajectory one [23]. In the latter the potential-energy barrier was located in $H + HBr$ channel and many of the systems were reflected back toward reactants before reaching the activated complex, when they struck (at high energies) the curved region of the reacting path in Fig. 2.5.

An asymmetric reaction has also been studied for three-dimensional systems and reasonable agreement was found between trajectory-calculated and activated-complex-theory-calculated results for forward (and, therefore, for reverse) reaction at the lower energies [24]. Even at the highest energies examined, the difference in reaction probability calculated from numerical trajectories and from activated-complex-theory results was only a factor of 2.

Quantum-mechanical comparisons of numerical solutions of the Schrodinger equation with actived-complex theory results for the reaction rate have been made only for the case of collinear collision [25, 26]. The $H + H_2$ reaction has been studied in this way. Activated-complex theory and vibrational adiabaticity were both tested [25], neglecting curvilinear effects in the definition of the vibrationally adiabatic model. The tunneling at low energies was greater in the exact results than in the adiabatic. An approximate estimate of the curvilinear effect [27] served to decrease the difference by a factor of about 2, but further detailed calculations on the curvilinearity should be performed. At the time of writing there are no quantum-mechanical results for three-dimensional systems of comparable accuracy.

In the field of unimolecular reactions there have been tests of activated-complex theory in a particular form, namely, tests [28–30] of the RRKM theory [31] of unimolecular reactions, a theory that blends the concepts formulated in the 1920s by Rice, Ramsperger, and Kassel with the later ideas embodied in activated-complex theory. Good agreement was found between numerical trajectory results on the dependence of lifetime of the high-energy unimolecularly decomposing molecule on its energy and RRKM theory [28, 29]. When there is only a weak potential-energy maximum near $s^\ddagger$, a minimum-density-of-states criterion, described in Section 5, was used to define a position of the activated complex [29].

5 LOCATION OF THE ACTIVATED COMPLEX AND THE POINT OF MAXIMUM FREE ENERGY

The position $s_n^\ddagger$ of the activated complex for any n was seen earlier to be that for which $V_1(s) + E_n(s)$ has its maximum value. When there are many states n or when inadequate information is available about the s dependence of each, the procedure of locating each $s_n^\ddagger$ is too formidable and resort must be made to some more approximate argument. Just as in a simpler system where $s^\ddagger$ is frequently chosen to occur at the maximum of $V_1(s)$, so too is the $s^\ddagger$ in these more complicated systems usually defined as the one occurring at the maximum of some free energy $A(s)$, in a plot of $A(s)$ versus s. In the present section we shall consider a basis for such a choice of s using (2.10)–(2.12).

We use $\epsilon_n(s)$ to denote the sum,

$$\epsilon_n(s) = E_n(s) + V_1(s). \tag{2.40}$$

By definition of $s_n^\ddagger$, one has

$$\epsilon_n(s) \leq \epsilon_n(s_n^\ddagger). \tag{2.41}$$

Thus, in (2.10)–(2.12)

$$Q_{\text{eff}}^\ddagger = \sum_n \exp\left[\frac{-\epsilon_n(s_n^\ddagger)}{kT}\right] \leq \sum_n \exp\left[\frac{-\epsilon_n(s)}{kT}\right]. \tag{2.42}$$

The first sum in (2.42) is the correct one, and we wish, therefore, to make the last sum approach the first as closely as possible. To do so, one must choose an s, $s^\ddagger$, which makes the last sum as small as possible. Since the sum is related to the free energy $A(s)$ of a system moving on a hypersurface, at a given s,

$$\exp\left[\frac{-A(s)}{kT}\right] = \sum_n \exp\left[\frac{-\epsilon_n(s)}{kT}\right], \tag{2.43}$$

this choice of $s = s^\ddagger$ also serves to locate the largest value of $A(s)$ in a plot of $A(s)$ versus s and so provides a basis for the approximate procedure.

This criterion for the choice of $s^\ddagger$ is also related to a minimum-state-density criterion for choosing $s^\ddagger$ in a microcanonical ensemble. The latter criterion has been useful in some unimolecular [29] and bimolecular reactions [32].

In the case of reactions in solution, (2.37)–(2.39) would be used instead of (2.10)–(2.12), but otherwise, the argument would completely parallel that in (2.40)–(2.43) and so provide a basis for the sometimes used procedure of maximizing $G^\ddagger(s)$ to define the $s^\ddagger$ in (2.39).

6 REMARKS ON APPLICATIONS

The many applications of activated-complex theory to reactions have been described in many texts [4, 9, 33]. They usually entail efforts to evaluate the partition function $Q^\ddagger$ from assumed properties of the potential-energy surface or to evaluate the free energy of activation $\Delta G^\ddagger$, sometimes using dielectric-continuum theory to treat ion-solvent interactions. In the present section we shall instead outline two applications that involve additional assumptions, namely, unimolecular reactions and electron-transfer reactions, in the first two parts. In the third, other reactions are discussed briefly, and in the fourth, the relation of activated complex to more dynamical properties is considered.

Unimolecular Reactions

In unimolecular reactions [31] one considers the activation and deactivation of energetic molecules of energy E, $A^*(E)$, by collisions with a molecule M, and reaction of those molecules,

$$\begin{aligned} \mathrm{A} + \mathrm{M} &\underset{k_{-1}}{\overset{k_1}{\rightleftharpoons}} \mathrm{A}^*(\mathrm{E}) + \mathrm{M} \\ \mathrm{A}^*(\mathrm{E}) &\xrightarrow[k_2]{} \text{products.} \end{aligned} \tag{2.44}$$

One considers all possible values of E that could lead to the reaction. Because of the second step in (2.44) the concentration of $\mathrm{A}^*(\mathrm{E})$ is below its equilibrium value, except when the concentration of M is high enough that the reverse step in step 1 dominates step 2 in (2.44). Such domination occurs at high enough pressure. Since $\mathrm{A}^*(\mathrm{E})$ is below its equilibrium value except at high pressures, activated-complex theory cannot be applied to the overall reaction in (2.44). Instead, it is applied in its microcanonical form to the second step to obtain the energy-dependent rate constant k_2 for that step. The energy-dependent rate constants k_1 and k_{-1} for the forward and reverse steps in step 1 are calculated by (a) noting that their ratio is the (microcanonical) equilibrium constant of that step at the given energy and (b) assigning some approximate value to the deactivation rate constant k_{-1}. One sums over E the contribution from $k_2\mathrm{A}^*(\mathrm{E})$ to obtain the overall reaction rate.

Sometimes, particularly with smaller systems, the moment of inertia of the activated complex in the second step of (2.44) is substantially larger than that of A^*. The resulting change in centrifugal potential in the second step influences k_2, and so, one considers the behavior of an ensemble of molecules of given E and rotational angular momentum $\mathbf{J}$, $\mathrm{A}^*(\mathrm{E}, \mathbf{J})$, finds their contribution to the reaction rate, and, finally, sums over all E and $\mathbf{J}$ [29, 31b, 34].

RRKM theory and its applications have been extensively discussed elsewhere [31, 35–37].

Electron-Transfer Reactions

Like the unimolecular reactions electron-transfer reactions [38] involve features additional to those contained in activated-complex theory. In certain respects, electron-transfer reactions are the simplest of all reactions: simple electron transfers involve no breaking of chemical bonds, no formation of new chemical bonds, but only fluctuations of bond lengths and bond angles and fluctuations of molecular orientations of the solvent in such a way as to facilitate electron transfer. The first problem is to define the nature of the activated complex for this electron transfer. Such a discussion leads to one of the potential-energy surfaces and to the role of the Franck-Condon principle in the electron transfer.

In any chemical reaction there is a change in configuration of the atoms and molecules from one that is appropriate to the reactants to one that is appropriate to the products. In reactions that involve only the transfer of an electron, there are the changes in configuration cited above: the bond lengths in a particular reactant will depend on the charge of that reactant and hence will differ before and after the electron-transfer step. Sometimes this difference is very small and may be ignored, but at other times it constitutes the principal factor making the electron-transfer rate constant small. Again, the solvent molecules in the vicinity of the reactant are more oriented, on the average, toward a more highly charged reactant. Thus, when the charge of that reactant is altered by electron transfer, the average degree of orientation of the solvent molecules around it eventually relaxes from the one appropriate to reactants to one appropriate to products. Thus, there is a net change in the distribution of orientations of many solvent molecules.

When the reactants are far apart, the reaction coordinate is the distance between the two particles. Gradually, as they come closer, the reaction coordinate begins to include the other kinds of motion discussed above—those involving fluctuations of bond lengths and bond angles in the coordination shells of the reactants and fluctuations of solvent-molecule reorientations. Along the reaction coordinate, such coordinates change from values appropriate to reactants to those appropriate to products. In this region, in fact, the reaction coordinate begins to resemble, instead of a translation, a vibrational-like motion as indicated schematically in Fig. 2.7.

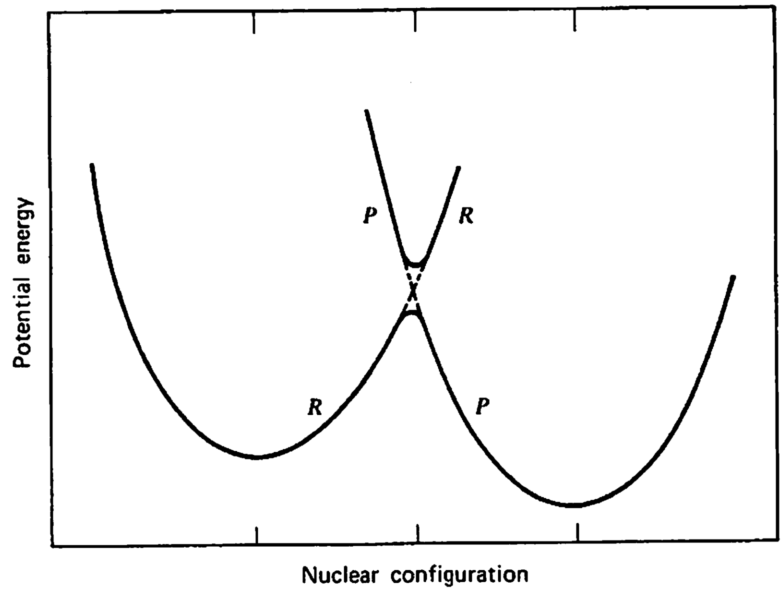

Fig. 2.7 Profile of potential-energy surfaces of reactants (*R*) and of products (*P*), plotted versus nuclear configuration of all the atoms in the system. --- = surface for zero electronic interaction of the reacting species. —— = adiabatic surface.

Figure 2.7 describes the profile, labeled *R*, of the many-dimensional surface of the potential energy of the two reactants and solvent, as a function of the various coordinates in the system mentioned above. It also contains a profile, labeled *P*, of the potential-energy surface of the products and solvent, as a function of the same coordinates. These two curves do not have minima at the same configuration, because the equilibrium bond lengths are different in any species when it is a reactant compared to when it is a product and because the typical favorable orientations of the solvent molecules are also different.

When the reactants are far apart, fluctuation in these coordinates can occur but without leading to an electron transfer, that is, without causing the system to move from curve *R* to curve *P* in Fig. 2.7. When the reactants are close together, there is appreciable electronic coupling between them, causing a splitting of these potential-energy surfaces, as indicated by the dotted lines in Fig. 2.7. Under such conditions a suitable fluctuation of coordinates from values appropriate to reactants toward values appropriate to products will lead in many cases to the system moving from the reactants curve to the products curve. For example, when the splitting of those surfaces is large enough, the system stays on the lowest split surface. That is, the system moves along the lower dotted line in Fig. 2.7. In this case the reaction is said to be adiabatic as far as the electronic motion is concerned. If, on the other hand, the splitting is very small, the chance of the system moving from the reactants' curve to the products' curve becomes correspondingly small, and on the occasions that it does so, the reaction is said to be electronically nonadiabatic.

For reaction to occur, we have seen that it is necessary for the system to reach the intersection region in Fig. 2.7. This need is another way of stating the Franck-Condon principle for this electron-transfer problem: The Franck-Condon principle states that the process of going from the *R* surface to the *P* surface in Fig. 2.7 is a "vertical" one, to avoid changing atomic positions (and momenta). Thus, if the electron transfer occurred to the left of the intersection region in Fig. 2.7, the transfer would require the absorption of light and thus be a photochemical reaction rather than a thermal reaction.

An important part of the problem of calculating the reaction rate lies in calculating the probability of reaching in this many-dimensional coordinate system the intersection of the two potential energy surfaces, *R* and *P*, in Fig. 2.7. If activated-complex theory is applied to this system, this intersection of the two surfaces constitutes, in effect, the activated complex for the reaction.

In applying activated-complex theory one circumstance that makes these reactions different from most other reactions involving ions in solution should be noted: In the electron-transfer reactions of the type discussed here ("outer sphere" electron transfers), there is a large separation distance between the charges of the reacting species before and after the transfer. In most other reactions the change of charge distribution does not occur as dramatically. This considerable change of charge distribution occurs in a relatively small increment of reaction coordinate in Fig. 2.7 as the system moves along the dotted line.

We consider the solvent polarization change accompanying the motion in Fig. 2.7. The actual many-dimensional surface, whose profile is approximated in Fig. 2.7, actually has many local minima (since solvent orientations do not obey harmonic oscillator laws of motion). The many configurations in the general vicinity of these minima, suitably weighted by a Boltzmann factor, contribute to the solvent dielectric polarization. The solvent polarization represented by any group of configurations on, or near, the intersection region in Fig. 2.7 cannot be in thermal equilibrium with the charges of the reactants (or with that of products). Thus, this polarization fluctuates from the equilibrium polarization appropriate to reactants as the system moves toward the intersection region in Fig. 2.7 and can be termed a *nonequilibrium polarization*. The electronic polarization of the system is typically, on the other hand, largely in equilibrium with the field created by the charges and by the remaining polarization (orientational, vibrational) of the solvent.

To calculate the free energy of a system containing this yet to be determined polarization function one has to find a reversible path for forming this nonequilibrium polarization system. Such a path was found by charging up the system to form the desired orientation-vibration polarization function of position and by holding that polarization fixed, changing the charges to the desired values (i.e., of reactants or of products), allowing the electronic polarization to adjust to these changes [38].

This expression for the free energy of the fluctuation involves an integral whose integrand is a quadratic function of the polarization (in the usual dielectric unsaturation approximation). One can minimize it to obtain the unknown polarization function, subject to the condition that the activated complex consists of configurations on the intersection of the R and P surfaces in Fig. 2.7. In this way the free energy of activation $\Delta G^{\ddagger}$ was calculated. The details have been described elsewhere [38]. Here, we give the functional form of the equations:

$$k_r = Z \exp\left(\frac{-\Delta G^{\ddagger}}{kT}\right) \tag{2.45}$$

$$\Delta G^{\ddagger} = w^r + \frac{\lambda}{4} + \frac{\Delta G^{0\prime}(R)}{2} + \frac{\Delta G^{0\prime}(R)^2}{4\lambda} \tag{2.46}$$

where Z is the collision frequency, w^r is the work required to bring the reactants to some most probable distance R in the activated complex, λ is an intrinsic reorganization property, and $\Delta G^{0'}(R)$ is the "standard" free energy of reaction* in the prevailing medium and at the separation distance R,

$$\Delta G^{0'}(R) = \Delta G^{0'} + w^p - w^r, \tag{2.47}$$

where w^p is the work required to bring the products together to the separation distance R.

λ has a certain additivity property: In the cross-reaction

$$\mathrm{A(ox)} + \mathrm{B(red)} \rightarrow \mathrm{A(red)} + \mathrm{B(ox)} \tag{2.48}$$

and isotopic-exchange reactions

$$\begin{aligned} \mathrm{A(ox)} + \mathrm{A^*(red)} &\rightarrow \mathrm{A(red)} + \mathrm{A^*(ox)} \\ \mathrm{B(ox)} + \mathrm{B^*(red)} &\rightarrow \mathrm{B(red)} + \mathrm{B^*(ox)}, \end{aligned} \tag{2.49}$$

with the λ written as λ_{ab}, λ_{aa}, λ_{bb}, respectively, we have [38]

$$\lambda_{ab} \cong \tfrac{1}{2}(\lambda_{aa} + \lambda_{bb}). \tag{2.50}$$

In the case of electrode reactions, $\Delta G^{\ddagger}$ is given by (2.46)–(2.47) but with λ replaced by a λ_{el} and with $\Delta G^{0'}$ replaced by the activation overpotential, ne$(E - E^{0'})$, E and $E^{0'}$ being the actual and "standard" potential for the system.

A variety of predictions result from these equations for reactions in solution and at electrodes have been the subject of many experimental tests. Among the predictions are the relation of isotopic-exchange rate constants to those for cross-reactions, the effect of the standard free energy ΔG^0 on reaction rates, the effect of the activation overpotential on the electrochemical reaction rate, and relations between rate constants of homogenous and electrochemical reactions. The results are described in various articles and reviews [39, 40].

Remarks on Other Reactions

The treatment of electron transfers in the previous section raises the question of whether analogous predictions can be made for other reactions (viz., atom and proton transfers). In the case of atom transfers the potential-energy surfaces are typically not of the small-splitting (weak-interaction) type in Fig. 2.7. Instead, the splitting is very large, and a different method of calculation must be used. While ab initio surfaces have been calculated for several chemical reactions [41], semiempirical surfaces will continue to be used for some time to come. One very simple method that has yielded

---

* That is, it is the free energy of any two *specified* product molecules, a distance R apart, minus that of the two *specified* reactant molecules at the same R. Thus, it contains no entropy-of-mixing term, and so is labeled "standard." The quotation marks refer to the fact that $\Delta G^{0'}$ is calculated for the prevailing temperature and medium, rather than for some standard state.

surprisingly reasonable results for activation energies of reactions has been the BEBO (bond-energy–bond-order) method [42].

With this method it has been possible to deduce an equation somewhat similar in form to the ones in the preceding subsection and to show that the slope of a Bronsted plot of $\Delta G^{\ddagger}$ versus ΔG^{0} is approximately equal to the bond order of the newly formed bond, in a reaction in which one bond was broken and a new one formed [43].

Apart from steric effects and statistical factors, which are included separately, $\Delta G^{\ddagger}$ is of the following form, based by analogy on the corresponding expression for $\Delta E^{\ddagger}$ for gas reactions [43],

$$\Delta G^{\ddagger} = w^{r} + \frac{\lambda}{4} + \frac{\Delta G^{0\prime}(R)}{2} + \frac{\Delta G^{0\prime}(R)}{2y} \ln \cosh y \tag{2.51}$$

$$y = \frac{2\,\Delta G^{0\prime}(R) \ln 2}{\lambda} \tag{2.52}$$

and λ again has the approximate additivity property (2.50). Applications of the equations to the data have been made [44, 45]. (But, the less rigorous nature of this approach as compared with that in the preceding subsection should be noted.)

The treatment of proton transfers has ingredients of both that of electron transfers and that of atom transfers. The theory for these reactions appears, therefore, to be more formidable than that for the other two. Depending upon the system, the proton might form such a strong bridge between the reactants that the rearrangement of charge distribution accompanying proton transfer will be relatively small. Or, when the bridge is weak, perhaps even sterically hindered [46], the change of charge distribution is more substantial and might require appreciable reorganization of the solvent, perhaps as in electron transfer. A number of investigations of these problems have been made and further work remains to be done because of the complexity of the problem [47]. Equations (2.46) and (2.51) have been applied to $\Delta G^{\ddagger}$ versus $\Delta G^{0\prime}$ data [44, 45].

To study the dependence of $\Delta G^{\ddagger}$ ln $\Delta G^{0\prime}$ in the reactions of the previous or present section, it is customary to hold one reagent fixed and vary the other reagent. Particular care is needed to choose a series in which λ does not also vary significantly in the series if one is to obtain the simplest results for interpretation. In such a case the intercept of a plot of $\Delta G^{\ddagger}$ versus $\Delta G^{0\prime}$ is $\frac{1}{2}(w^{r} + w^{p}) + (\lambda/4)$. When the w-terms either are small or can be estimated, λ can be calculated [44, 45].

In the case of proton transfers, with A referring to a nitrogen base or acid to an oxygen base or acid, rather than a carbon acid or base, the λ_{aa} is very small. Variation in A in a series leaves λ_{aa} and hence the λ in (2.50) largely unchanged during the series and leads to a simple $\Delta G^{\ddagger}$ versus $\Delta G^{0'}$ plot. In contrast, when the varying reagent is a carbon acid or base, λ varies and anomalous values [48] (negative or greater than unity) are found for the slope of $\Delta G^{\ddagger}$ versus $\Delta G^{0'}$ plots. The slopes found in the other small λ_{aa} case have the expected values between zero and unity, varying from zero at sufficiently negative $\Delta G^{0'}$ to unity at sufficiently positive $\Delta G^{0'}$. In applications to the data, the slope has been typically 0.5 at small $\Delta G^{0'}$ or less than 0.5 for quite negative $\Delta G^{0'}$ and greater than 0.5 at quite positive $\Delta G^{0'}$ as expected from (2.46) or (2.51) [44].

Exit or Entrance Channel States and Activated-Complex States

With the increasing development of new experimental methods, including gas-phase studies with molecular beams or infrared chemiluminescence of rotationally and vibrationally excited products [49], there has been a need for theories capable of predicting or interpreting the increased dynamical information. The principal theoretical technique used thus far for such studies is a classical mechanical treatment of the coordinates describing the collision. Hamilton's equations of motion for the coordinates and momenta are integrated numerically, using initial conditions and initial distributions appropriate to the experiment, and the distribution of final values of observables are determined and compared with experiment [19].

Quantum effects can occur in such reactions, typically in a "threshold region," a region where probability of formation of some final quantum state of products changes rapidly with energy or with quantum state. However, fully three-dimensional numerical and accurate quantum-mechanical calculations have not yet been made for even the simplest chemical reaction, although several groups are now developing a method. The recent development of "exact semiclassical" methods for treating molecular collisions may bridge this gap [50, 51].

For some reactions it has been possible to develop analytical models, such as for "spectator-stripping" reactions [52] and for reactions involving long-lived complexes [53]. The question arises as to whether extra assumptions can be added to activated-complex theory so that it, too, can deal with the more dynamical problems—problems such as dependence of the probability of reaction and reaction cross section on initial velocity and quantum state of the reactants and such as the probability distribution for formation of products in various final quantum states and with specified range of final velocities. We mention below several recent efforts to treat these problems.

For reactions (2.1) that are vibrationally adiabatic insofar as the stretching vibration is concerned (the r-coordinate in Fig. 2.6) and for which the other internal coordinates are statistically vibrationally adiabatic, from reactants to activated complex, it has been possible to use microcanonical activated-complex theory to develop a treatment of reaction cross sections [54, 55]. Agreement with trajectory data on the H + H_2 exchange reaction was quite reasonable at energies of interest for the thermal reaction.

On the other hand, appreciably endothermic reactions are typically highly nonadiabatic according to data on the reverse exothermic reaction [56], and the above method would not be applicable. A method has been described for representing phenomenologically the extensive data [57, 58] and represents a stimulating approach.

Recently, molecular beam techniques have been used to measure translational energy distributions of reactions involving complexes [53, 59, 60]. The results of such studies have been compared with RRKM-type theory. In such a theory predictions can be made regarding translational distribution *in the activated complex*. They can be made [60] for that of the *final products* only in the case of a truly "loose" activated complex for the exit channel of the reaction (a complex in which the product molecules exist and rotate freely), as it appears to be in Ref. [53]. (Such a remark applies in general to the calculation of the translational distribution of the products from that in the activated complex.) In other cases, added assumptions are needed to make such predictions, and thus, one tests not simply RRKM but RRKM plus added assumptions [61].

One result of many of these more dynamical experimental and theoretical studies is that more and more information is becoming available on the reactions themselves, on the shape of the activated complexes [62], and on the nature of the potential-energy surfaces—"early" of "late downhill," and so on [56]. Such information supplements the quite different type of information obtained by the more classical methods used for reactions in solution and in the gas phase, as well as providing data vital to understanding nonequilibrium reactive systems in such environments as lasers, the upper atmosphere, and, presumably, interstellar space.

Other interesting studies that should be noted but that have not been discussed above include phase-space theory [63], which aims at discussing distributions without reference to the potential-energy surface and contributions to a more formal theory of kinetics [64]. Excellent detailed reviews have appeared on various quantum mechanical aspects of inelastic and reactive collisions [65]. A recent symposium and review [66] may also be consulted in this regard.

Acknowledgment

I am particularly indebted to my co-worker, Dr. Richard Ellis, for his helpful comments. Research on which some of the material in this chapter was based was supported by a grant from the National Science Foundation.

References

1. Compare H. Eyring, J. Walter, and G. E. Kimball, *Quantum Chemistry*, Wiley, New York, 1944, Chap. 16.
2. M. A. Eliason and J. O. Hirschfelder, *J. Chem. Phys.*, **30,** 1426 (1959).
3. R. A. Marcus, *J. Chem. Phys.*, **43,** 1598 (1965).
4. S. Glasstone, K. J. Laidler, and H. Eyring, *The Theory of Rate Processes*, McGraw-Hill, New York, 1941, esp. p. 260 and Chap. 3.
5. E. Gorin, *Acta Physiochim. U.R.S.S.*, **9,** 681 (1938).
6. F. T. Smith, *J. Chem. Phys.* **31,** 1352 (1959). Subsequent change of μ by a factor of, say, f merely rescales the mass-weighted coordinates by $1/\sqrt{f}$.
7. R. P. Bell, *Trans. Faraday Soc.*, **55,** 1 (1959).
8. Curvilinear effects on transmission coefficients were also considered many years ago for discontinuous potential energy surfaces by H. M. Hulbert and J. O. Hirschfelder, *J. Chem. Phys.*, **11,** 276 (1943); and D. W. Jepsen and J. O. Hirschfelder *ibid.*, **30,** 1032 (1959).
9. See, for example, K. J. Laidler, *Theories of Chemical Reaction Rates*, McGraw-Hill, New York, 1969, Chap. 8 and references cited therein; and B. Shizgal, *J. Chem. Phys.*, **55,** 76 (1971).
10. J. O. Hirschfelder and E. Wigner, *J. Chem. Phys.*, **7,** 616 (1939), esp. p. 624.
11. R. A. Marcus, *J. Chem. Phys.*, **45,** 4493, 4500 (1966).
12. R. A. Marcus, *J. Chem. Phys.*, **49,** 2610, 2617 (1968).
13. L. Hofacker, *Z. Naturforsch., A*, **18,** 607 (1963).
14. R. A. Marcus, *J. Chem. Phys.*, **41,** 2614, 2624 (1964).
15. M. S. Child, *Disc. Faraday Soc.*, **44,** 68 (1967).
16. Compare S. F. Wu and R. A. Marcus, *J. Chem. Phys.*, **53,** 4026 (1970), cf. eq. (14) and Fig. 12; and R. A. Marcus, *Disc. Faraday Soc.*, **44,** 7 (1967).
17. Compare R. B. Bernstein, A. Dalgarno, H. S. W. Massey, and I. C. Percival, *Proc. Roy. Soc.* (London), **A274,** 427 (1963); and W. A. Lester, Jr., and R. B. Bernstein, *J. Chem. Phys.*, **53,** 11 (1970), regarding a statistical distribution in a related problem of collisional rotational-translational energy transfer in a strong coupling regime.
18. T. L. Hill, *Statistical Mechanics*, McGraw-Hill, New York, 1956, p. 75.
19. D. L. Bunker in B. Alder, S. Fernbach, and M. Rotenberg, Eds., *Methods in Computational Physics*, Vol. X, Academic, New York, 1971, p. 287; D. L. Bunker, in C. Schlier, Ed., *Molecular Beams and Reaction Kinetics*, Academic, New York, 1970, p. 355 and references cited therein; and M. Karplus, *ibid.*, p. 372 and references cited therein.
20. M. Karplus, R. N. Porter, and R. D. Sharma, *J. Chem. Phys.*, **43,** 3259 (1965). This reference also contains a comparison of classical trajectory results with a quantum activated-complex theory.
21. R. A. Marcus, *J. Chem. Phys.*, **45,** 2138 (1966).
22. K. Morokuma, B. C. Eu, and M. Karplus, *J. Chem. Phys.*, **51,** 5193 (1969).
23. K. Morokuma and M. Karplus, *J. Chem. Phys.*, **55,** 63 (1971).
24. G. W. Koeppl and M. Karplus, *J. Chem. Phys.*, **55,** 4667 (1971).

25. E. M. Mortensen, *J. Chem. Phys.*, **48,** 4029 (1968); D. G. Truhlar and A. Kuppermann, *ibid.*, **56,** 2232 (1972); and references cited therein.
26. D. J. Diestler, D. G. Truhlar, and A. Kuppermann, *Chem. Phys. Lett.*, **13,** 1 (1972).
27. Do Ren Chang and R. A. Marcus, unpublished calculations.
28. D. L. Bunker, *J. Chem. Phys.*, **37,** 393 (1962).
29. D. L. Bunker and M. Pattengill, *J. Chem. Phys.*, **48,** 772 (1968).
30. P. Brumer and M. Karplus, *Disc. Faraday Soc.*, **55,** (1973). Table 2.
31. (a) R. A. Marcus and O. K. Rice, *J. Phys. Colloid Chem.*, **55,** 894 (1951); R. A. Marcus, *J. Chem. Phys.*, **20,** 359 (1952); (b) *ibid.*, **43,** 2658 (1965); *ibid.*, **52,** 1018 (1970).
32. W. H. Wong and R. A. Marcus, *J. Chem. Phys.*, **55,** 5625 (1971).
33. E.g., R. E. Weston, Jr. and H. A. Schwarz, *Chemical Kinetics*, Prentice-Hall, Englewood Cliffs, N.J., 1972; A. A. Frost and R. G. Pearson, *Kinetics and Mechanism*, 2nd ed., Wiley, New York, 1961; H. S. Johnston, *Gas-Phase Reaction Rate Theory*, Ronald, New York, 1966; and S. W. Benson, *The Foundations of Chemical Kinetics*, McGraw-Hill, New York, 1960.
34. E. V. Waage and B. S. Rabinovitch, *Int. J. Chem. Kinet.*, **3,** 105 (1971) and references cited therein.
35. B. S. Rabinovitch and M. C. Flowers, *Quart. Rev.*, **18,** 122 (1964); L. D. Spicer and B. S. Rabinovitch, *Ann. Rev. Phys. Chem.*, **21,** 349 (1970); E. A. Hardwidge, B. S. Rabinovitch, and R. C. Ireton, *J. Chem. Phys.*, **58,** 340 (1973); P. J. Robinson and K. A. Holbrook, *Unimolecular Reactions*, Wiley, New York, 1972.
36. D. W. Setser in J. C. Polanyi, Ed., *MTP International Review of Science, Phys. Chem. Ser. 1, Vol. IX, Chemical Kinetics*, Butterworths, London, 1972, Chapter 1.
37. R. A. Marcus, in H. Hartmann, Ed., *Chemische Elementarprozesse*, Springer, Berlin, 1968, p. 109ff.
38. R. A. Marcus, *J. Chem. Phys.*, **24,** 966 (1956); *Disc. Faraday Soc.*, **29,** 21 (1960); *J. Phys. Chem.*, **67,** 853, 2889 (1963); *Ann. Rev. Phys. Chem.*, **15,** 155 (1964); *J. Chem. Phys.*, **43,** 679 (1965); *Electrochim. Acta*, **13,** 995 (1968); and Ref. 37, p. 348.
39. N. Sutin, *Ann. Rev. Phys. Chem.*, **17,** 119 (1966); W. L. Reynolds and R. W. Lumry, *Mechanisms of Electron Transfer*, Ronald, New York, 1966; R. E. Weston, Jr. and H. A. Schwarz, Ref. 33, p. 205ff; R. P. Wayne, in C. H. Bamford and C. F. H. Tipper, Eds., *Comprehensive Chemical Kinetics, Vol. II: The Theory of Kinetics*, Elsevier, Amsterdam, 1969, p. 338ff; T. J. Meyer and H. Taube, *Inorg. Chem.*, **7,** 2369 (1968); R. G. Wilkins and R. E. Yelin, *ibid.*, **7,** 2667 (1968); M. E. Peover and J. S. Powell, *J. Electroanal. Chem.*, **20,** 427 (1969); K. Höfelmann, J. Jagur-Grodzinski, and M. Szwarc, *J. Am. Chem. Soc.*, **91,** 4645 (1969); J. R. Brandon and L. M. Dorfman, *J. Chem. Phys.*, **53,** 3849 (1970); D. Rehm and A. Weller, *Israel J. Chem.*, **8,** 259 (1970); N. Winograd and T. Kuwana, *J. Am. Chem. Soc.*, **93,** 4343 (1971); J. R. Pladziewicz and J. H. Espenson, *J. Phys. Chem.*, **75,** 3381 (1971); N. Sutin in G. L. Eichorn, Ed., *Inorganic Biochemistry*, Elsevier, Amsterdam (in press), Chapter 19; J. M. Hale, in N. S. Hush, Ed., *Reactions of Molecules at Electrodes*, Wiley, New York, 1971, p. 229ff; and R. A. Marcus, in P. Kirkov, Ed., *Quantum Mechanical Aspects of Electrochemistry, Proceedings of the I Session of International Summer School on Quantum Mechanical Aspects of Electrochemistry*, Center for Radioisotope Application, Skopje, Yugoslavia, 1971, p. 44ff. For

exceptions involving cobalt systems, see G. Davies and B. Warnquist, *Coord. Chem. Rev.*, **5**, 349 (1970).

40. For review of related approaches, see V. G. Levich, *Adv. Electrochem. Eng.*, **4**, 249 (1966); V. G. Levich, in H. Eyring, D. Henderson, and W. Jost, Eds., *Physical Chemistry, Vol. IXB: Electrochemistry*, 1970, Chapter 12; R. R. Dogonadze in *Reactions of Molecules at Electrodes*, Wiley, New York, 1971, p. 135ff; and A. J. Appleby, J. O'M. Bockris, and R. K. Sen, in J. O'M. Bockris, Ed., *MTP International Review of Science, Physical Chemistry Ser. 1, Vol. VI: Electrochemistry*, Butterworths, 1973, p. 1ff.
41. See, for example, I. Shavitt, *J. Chem. Phys.*, **49**, 4048 (1968); and S. V. O'Neil, P. K. Pearson, H. F. Schaefer, and C. F. Bender, *ibid.*, **58**, 1126 (1973).
42. H. S. Johnston, Ref. 33.
43. R. A. Marcus, *J. Phys. Chem.*, **72**, 891 (1968).
44. A. O. Cohen and R. A. Marcus, *J. Phys. Chem.*, **72**, 4249 (1968); and R. A. Marcus, *J. Am. Chem. Soc.*, **91**, 7224 (1969).
45. J. Hine, *J. Am. Chem. Soc.*, **93**, 3701 (1971); and M. M. Kreevoy and D. E. Konasewich, *Adv. Chem. Phys.*, **21**, 243 (1971).
46. E. S. Lewis and L. H. Funderbunk, *J. Am. Chem. Soc.*, **89**, 2322 (1967); R. P. Bell and D. M. Goodall, *Proc. Roy. Soc.* (London), **A294**, 273 (1966).
47. See, for example, M. Eigen, *Disc. Faraday Soc.*, **39**, 7 (1965); R. P. Bell, *ibid.*, **39**, 16 (1965); R. P. Wayne, Ref. 39, pp. 345ff; J. L. Kurz and L. C. Kurz, *J. Am. Chem. Soc.* **94**, 4451 (1972); J. Albery, *Progr. Reaction Kinet.*, **4**, 353 (1967); V. G. Levich, R. R. Dogonadze, and A. M. Kuznetsov, *Electrochim. Acta*, **13**, 1025 (1968); M. A. Vorotyntsev, R. R. Dogonadze, and A. M. Kuznetsov, *Dokl. Phys. Chem. I*, **195**, 948 (1970) and references cited therein; and A. J. Appleby, J. O'M. Bockris, and R. K. Sen, Ref. 40.
48. F. G. Bordwell and W. J. Boyle, Jr., and K. C. Yee, *J. Am. Chem. Soc.*, **92**, 5926 (1970); and R. A. Marcus, *ibid.*, **91**, 7224 (1969).
49. See reviews by T. Carrington and J. C. Polanyi, and by J. L. Kinsey, in Ref. 36, Chapters 5 and 6, respectively.
50. R. A. Marcus, *Chem. Phys. Lett.*, **7**, 525 (1970); and *Disc. Faraday Soc.*, **55**, 34 (1973) and references cited therein.
51. W. H. Miller, *J. Chem. Phys.*, **53**, 1949, 3578 (1970); and W. H. Miller and A. W. Raczkowski, *Disc. Faraday Soc.*, **55**, (1973) and references cited therein.
52. See, for example, A. Henglein, K. Lacmann, and B. Knoll, *J. Chem. Phys.*, **43**, 1048 (1965); and R. E. Minturn, S. Datz, and R. L. Becker, *ibid.*, **44**, 1149 (1966).
53. W. B. Miller, S. A. Safron, and D. R. Herschbach, *Disc. Faraday Soc.*, **44**, 108 (1967).
54. R. A. Marcus, *J. Chem. Phys.*, **45**, 2630 (1966); and *ibid.*, **46**, 959 (1966).
55. For another example of the application of microcanonical activated-complex theory plus added assumptions to a different problem—the deduction of state-selected information for an endothermic reaction from data on the reverse reaction—see R. A. Marcus, *J. Chem. Phys.*, **53**, 604 (1970); cf. K. G. Anlauf, D. H. Maylotte, J. C. Polanyi, and R. B. Bernstein, *ibid.*, **51**, 5716 (1969).
56. For review, see T. Carrington and J. C. Polanyi, in Ref. 36, Chapter 5.
57. A. Ben Shaul, R. D. Levine, and R. B. Bernstein, *Chem. Phys. Lett.*, **15**, 160 (1972);

J. Chem. Phys., **57**, 5427 (1972); R. B. Bernstein and R. D. Levine, *Disc. Faraday Soc.*, **55**, (1973); and R. D. Levine, B. R. Johnston, and R. B. Bernstein, *Chem. Phys. Lett.*, **19**, 1 (1973).

58. G. L. Holacker and R. D. Levine, *Chem. Phys. Lett.*, **15**, 165 (1972); and *ibid.*, **9**, 617 (1971).
59. J. M. Parson and Y. T. Lee, *J. Chem. Phys.*, **56**, 4658 (1972); and Y. T. Lee, J. M. Parson, S. A. Rice, and K. Shobotake, *Disc. Faraday Soc.*, **55**, (1973).
60. S. A. Safron, N. D. Weinstein, and D. R. Herschbach, *Chem. Phys. Lett.*, **12**, 564 (1972); and D. L. King and D. R. Herschbach, *Disc. Faraday Soc.*, **55**, (1973; D. R. Herschbach, *ibid*, **55**, (1973).
61. cf. R. A. Marcus, *Disc. Faraday Soc.*,**55**, (1973); D. R. Herschbach, *ibid.*, **55**, (1973).
62. J. D. McDonald, P. R. LeBreton, Y. T. Lee, and D. R. Herschbach, *J. Chem. Phys.*, **56**, 769 (1972); and D. R. Herschbach, in W. A. Lester, Jr., Ed., *Proceedings of the Conference on Potential Energy Surfaces*, IBM Research Laboratory, San Jose, Calif., 1971.
63. P. Pechukas and J. C. Light, *J. Chem. Phys.*, **42**, 3281 (1965); and J. C. Light, *Disc. Faraday Soc.*, **44**, 14 (1967); compare J. Keck, *J. Chem. Phys.*, **29**, 410 (1958).
64. See, for example, J. Ross and J. Mazur, *J. Chem. Phys.*, **35**, 19 (1961); B. C. Eu and J. Ross, *ibid.*, **44**, 2467 (1966); F. H. Mies and M. Krauss, *J. Chem. Phys.*, **45**, 4455 (1966); F. H. Mies, *ibid.*, **51**, 787, 798 (1969); O. K. Rice, *ibid.*, **55**, 439 (1972); R. A. van Santen, *ibid.*, **57**, 5418 (1972); and T. F. George and J. Ross, *ibid.*, **56**, 5786 (1972) and references cited therein.
65. R. D. Levine, in W. B. Brown, Ed., *MTP International Review of Science, Vol. I, Theoretical Chemistry*, Butterworths, London, 1972, p. 229ff; T. F. George and J. Ross, *Ann. Rev. Phys. Chem.*, **24**, 263 (1973); and D. Secrest, *ibid.*, **24**, 379 (1973).
66. R. A. Marcus, *Disc. Faraday Soc.*, **55**, 9 (1973).